4-8-2010

High Frequency Acceleration Feedback Significantly Increases the Realism of Haptically Rendered Textured Surfaces

William McMahan
University of Pennsylvania, wmcmahan@seas.upenn.edu

Joseph M. Romano
University of Pennsylvania, jrom@seas.upenn.edu

Amal M. Abdul Rahuman
University of Pennsylvania, rahuman@seas.upenn.edu

Katherine J. Kuchenbecker
University of Pennsylvania, kuchenbe@seas.upenn.edu

Suggested Citation:
McMahan, William, Joseph M. Romano, Amal M. Abdul Rahuman and Katherine J. Kuchenbecker. (2010). *High frequency acceleration feedback significantly increases the realism of haptically rendered textured surfaces.* Haptics Symposium, 2010. Waltham, Massachusetts. March 25-26, 2010.

High Frequency Acceleration Feedback Significantly Increases the Realism of Haptically Rendered Textured Surfaces

Abstract

Almost every physical interaction generates high frequency vibrations, especially if one of the objects is a rigid tool. Previous haptics research has hinted that the inclusion or exclusion of these signals plays a key role in the realism of haptically rendered surface textures, but this connection has not been formally investigated until now. This paper presents a human subject study that compares the performance of a variety of surface rendering algorithms for a master-slave teleoperation system; each controller provides the user with a different combination of position and acceleration feedback, and subjects compared the renderings with direct tool-mediated exploration of the real surface. We use analysis of variance to examine quantitative performance metrics and qualitative realism ratings across subjects. The results of this study show that algorithms that include high-frequency acceleration feedback in combination with position feedback achieve significantly higher realism ratings than traditional position feedback alone. Furthermore, we present a frequency-domain metric for quantifying a controller's acceleration feedback performance; given a constant surface stiffness, the median of this metric across subjects was found to have a significant positive correlation with median realism rating.

Disciplines

Engineering | Mechanical Engineering

Comments

Suggested Citation:
McMahan, William, Joseph M. Romano, Amal M. Abdul Rahuman and Katherine J. Kuchenbecker. (2010). *High frequency acceleration feedback significantly increases the realism of haptically rendered textured surfaces.* Haptics Symposium, 2010. Waltham, Massachusetts. March 25-26, 2010.

High Frequency Acceleration Feedback Significantly Increases the Realism of Haptically Rendered Textured Surfaces

William McMahan[*] Joseph M. Romano[†] Amal M. Abdul Rahuman[‡] Katherine J. Kuchenbecker[§]

Haptics Group, GRASP Laboratory
University of Pennsylvania, USA

Abstract

Almost every physical interaction generates high frequency vibrations, especially if one of the objects is a rigid tool. Previous haptics research has hinted that the inclusion or exclusion of these signals plays a key role in the realism of haptically rendered surface textures, but this connection has not been formally investigated until now. This paper presents a human subject study that compares the performance of a variety of surface rendering algorithms for a master-slave teleoperation system; each controller provides the user with a different combination of position and acceleration feedback, and subjects compared the renderings with direct tool-mediated exploration of the real surface. We use analysis of variance to examine quantitative performance metrics and qualitative realism ratings across subjects. The results of this study show that algorithms that include high-frequency acceleration feedback in combination with position feedback achieve significantly higher realism ratings than traditional position feedback alone. Furthermore, we present a frequency-domain metric for quantifying a controller's acceleration feedback performance; given a constant surface stiffness, the median of this metric across subjects was found to have a significant positive correlation with median realism rating.

Index Terms: H.1.2 [Models and Principles]: User/Machine Systems—Human Information Processing; H.5.1 [Information Interfaces and Presentation]: Multimedia Information Systems—Artificial, augmented, and virtual realities; H.5.2 [Information Interfaces and Presentation]: User Interfaces—Haptic I/O

1 Introduction

Typical kinesthetic haptic interfaces provide the user with a handheld tool through which one can touch virtual or remote objects. Most of these devices are lightweight backdriveable robot arms, such as the Sensable Phantom Omni. These impedance-type systems measure the movement of the tool with position sensors and use actuators to output forces in response. An important goal in haptics is to make interactions with artificially rendered surfaces indistinguishable from tool-mediated contact with real physical objects. The traditional approach to haptic rendering uses virtual springs and dampers to connect the handheld tool with a proxy on the surface of the virtual object, or with the measured location of the teleoperated robot's end effector. These traditional methods do a reasonable job of recreating the low frequency kinesthetic forces of interaction, and thus they can convey the general shape of objects; however, virtual springs and dampers act as a low-pass filter, leaving haptic surfaces rendered in this way feeling unrealistically soft and smooth.

[*]e-mail: wmcmahan@seas.upenn.edu
[†]e-mail: jrom@seas.upenn.edu
[‡]email: rahuman@seas.upenn.edu
[§]e-mail: kuchenbe@seas.upenn.edu

IEEE Haptics Symposium 2010
25 - 26 March, Waltham, Massachusetts, USA
978-1-4244-6822-5/10/$26.00 ©2010 IEEE

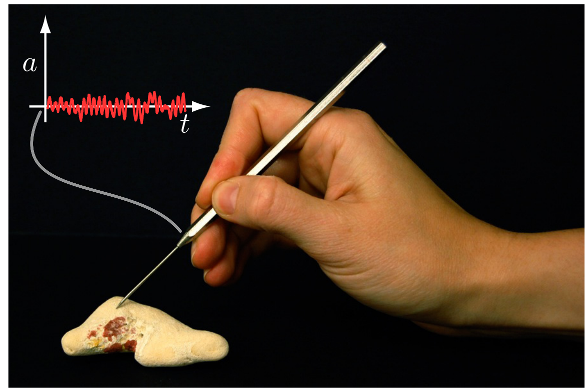

Figure 1: Tool-mediated interaction with real objects often produce strong high-frequency accelerations that allow one to determine key surface properties.

As shown in Fig. 1, the haptic sensations that mark real tool-mediated activities are both kinesthetic (low frequency forces) and vibrotactile (high frequency accelerations). Previous work, summarized in Section 2, suggests that high frequency acceleration feedback can improve the perceived realism of haptically rendered surfaces. Inspired by these findings, we recently developed a new method for feeding back high frequency accelerations, employing a dedicated voice-coil actuator and a dynamic model of the system [9, 12]. This paper describes the human subject study we conducted to quantify the realism benefit that can be attained by adding vibrotactile feedback to traditional surface renderings. We hypothesize that this addition will significantly improve the perceived realism of haptic interactions.

At first glance, the reported study is similar to those of [7] and [8], but several characteristics distinguish these works from one another. Our tested acceleration feedback method is novel in its use of a dedicated actuator, and our study employs a teleoperation system rather than synthetic virtual surfaces. Furthermore, the current study focuses on tangential surface exploration (dragging), while these previous studies were limited to simple tapping interactions.

Section 3 describes the specific hardware and haptic surface rendering algorithms that were used in this study. Section 4 describes the experimental protocol and outlines the subject's experience. Subsequently, we present the results of the experiment in Section 5 and discuss the implications of the results in Sections 6 and 7.

2 Background

Human perception of surface properties is an intricate and complex phenomenon that is not yet completely understood. What is known is that perception is informed by the stimulation of a variety of mechanoreceptors embedded in the skin, muscles, tendons, and joints. Each mechanoreceptor type responds best to a particular type of stimulation. Of particular relevance to tool-mediated haptic texture perception are the Pacinian corpuscles, which detect vibrotactile stimuli in the form of high frequency accelerations from approximately 20 Hz to 1000 Hz . These mechanoreceptors have broad receptive fields and are most responsive at 250 Hz [2].

As mentioned above, tool-mediated interactions with real objects cause the user to perceive both low frequency forces and high frequency accelerations. When humans are asked to determine a mechanical property of a surface (e.g., hardness or texture), they will select one of several typical exploratory motions, which are believed to make the target property easier to discern [10]. For example, when subjects are asked to determine the hardness of a surface, they tend to tap on the surface, and when asked to determine the roughness of a surface, they perform a tangential scanning motion. These findings motivate the need for high frequency acceleration feedback in haptic surface renderings and indicate that their absence may be a major cause for the unnatural feeling of many current haptic interfaces.

Traditional haptic surface renderings typically fail to reproduce high frequency accelerations for several reasons. In principle, the traditional virtual spring-damper surface rendering methods should be able to reproduce high frequency signals by increasing the spring stiffness and damping coefficient. Unfortunately physical limitations including servo rate, sensor resolution, quantization, and coulomb friction preclude stable closed-loop control at high stiffnesses or damping, thereby limiting systems to much lower values [5, 8]. A common negative side effect of this problem is unstable surface renderings, which generate a high frequency buzz that causes the surface to feel active [4]. Additionally, while commercially available devices have been optimized for low frequency kinesthetic force feedback, they are ill suited for the display of high frequency acceleration feedback. Factors including sampling rate, sensor resolution, amplifier nonlinearities, and device dynamics limit the bandwidth of the acceleration feedback they are capable of providing [3, 8, 14, 15]. As a result, naive attempts to exceed these limitations result in distortion and attenuation of the desired high frequency feedback.

Researchers have taken two approaches to overcoming these limitations. These approaches involve either more sophisticated control of the haptic device's actuators, or modifications to the design of the haptic display hardware. Okamura and colleagues [13] modeled contact accelerations as decaying sinusoidal waveforms with tuned parameters based upon real data. They rationalized that because the Pacinian corpuscles have a peak sensitivity of 250 Hz, there was no need to display accelerations much greater than this frequency. Thus, the parameters of these models were expertly scaled down so that they could be more faithfully recreated by their haptic device, a 3GM. These parameters were then further tuned based upon their subjective feel using data from a human subject experiment. Under this approach, users were able to distinguish three different virtual surfaces that differed by vibration alone. Anecdotally, users commented that while the surfaces did not feel exactly "real," the inclusion of the accelerations improved realism. The obvious drawback of this approach is that it requires extensive testing and subjective hand tuning in order to determine the appropriate parameters for a given surface.

Kuchenbecker and colleagues [7, 8] similarly chose to utilize the native hardware of a Sensable Phantom Premium 1.0 in order to recreate the contact accelerations of tapping on surfaces. In order to increase the fidelity with which they displayed high frequency feedback, they employed high quality linear current amplifiers and developed a dynamic model of their entire haptic system, including the influence of the user's hand. Their model carefully captured the high frequency response of their system, and by inverting this model they were able to provide the haptic device with the appropriate control to adequately track their desired feedback signals. When this method was tested in a human subject study, it achieved a significant improvement in the median realism ratings from 2 to 6 out of 7, where 7 indicates indistinguishable from the real surface. Unfortunately, the high frequency dynamics of most haptic systems are highly configuration dependent, and accounting for all of this variation requires a complex model that would be difficult to invert for real time control. Kuchenbecker and Niemeyer extended this approach to enable vertical tapping in a teleoperation system, but they did not report quantitative performance metrics or test with human subjects.

When grappling with similar performance limitations, Campion and Hayward designed their own high bandwidth haptic feedback device, the Pantograph Mark-II [3]. By using direct drive motors connected to stiff linkages, the authors were able to create a two-degree-of-freedom device with high frequency bandwidth capabilities. The device was then used to create fine virtual gratings.

Another viable approach is to augment existing haptic devices with an auxillary actuator that induces accelerations on the user's hand. Kontarinis and Howe [6] employed this approach by mounting inverted audio speakers to their custom haptic device near the user's fingertips. These speakers were driven by constant gain amplification of accelerations recorded from a teleoperated slave system. In subject trials, users showed improved performance in some tasks and anecdotally reported that they preferred the feel of the haptic display when it provided high frequency feedback..

Wall and Harwin designed a specialized handle for a Phantom Premium which featured a dedicated voice coil actuator, springs, and a linear position sensor [15]. The actuator was located between the hand and the Phantom endpoint. Using this handle they were able to feed back small amplitude high frequency positions to the user. This improved position tracking significantly increased subjects' ability to determine the orientation of virtual gratings. One problem they did note is that their design places an additional compliance between the user's hand and the haptic interface, thereby reducing the maximum stiffness renderable.

Our approach, described in [9] and [12], similarly advocates the use of a specialized handle fitted with a dedicated linear voice coil actuator and recentering springs. However, our design differs significantly from Wall and Harwin's because we choose to directly control the acceleration of the user's hand rather than the position of their hand. In our design the handle is rigidly attached to the haptic device's endpoint, and a spring-centered voice-coil actuator is embedded inside the handle. Thus, this design avoids placing additional compliant elements between the user and the haptic device, thereby maintaining the maximum stiffness displayable by our system. In comparison with Kontarinis and Howe, we use a higher performance actuator and we make a more concerted effort to perfectly match the accelerations recorded by the teleoperated slave. To acheive this goal we use frequency domain techniques to identify the high frequency dynamics of the haptic system. We utilize an approximate inversion of these high frequency dynamics in an open-loop controller to more faithfully render desired high frequency accelerations. Results in [9] and [12] show an improvement in acceleration matching from traditional position-position control. We have additional anecdotal evidence from public demonstrations to indicate that this approach improves the realism of rendered surfaces [11].

The human subject study described in this paper was designed to experimentally verify the anecdotal claims that high frequency acceleration feedback indeed improves the perceived realism of rendered textured surfaces. Additionally, it gives us an opportunity to evaluate the performance and robustness of our system with a variety of different users.

3 Experimental Setup

This study uses a modified version of the teleoperation setup presented in [9, 12]. As shown in Fig. 2 and described in more detail below, the master and slave are both Sensable Phantom Omni haptic

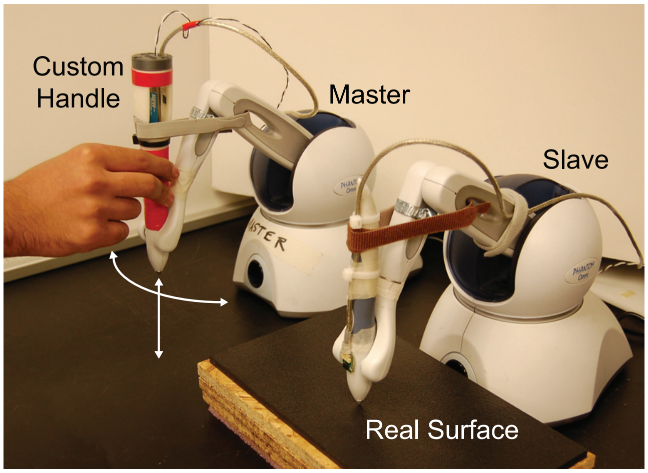

Figure 2: Our master-slave Phantom Omni setup with the modified master handle that contains a voice coil actuator. The master device is constrained to move along the two degrees of freedom shown. In this trial the real surface was placed underneath the slave device, and the user felt interaction forces through the teleoperation connection.

devices. The end effector of each device is fitted with an accelerometer, and a custom handle is attached to the master Omni to provide the user with high frequency acceleration feedback. We used this setup to develop eight different control algorithms that enable the operator to explore a real surface while feeling different types of haptic feedback.

3.1 Hardware

The master Omni's custom handle contains an NCM02-05-005-4JB linear voice coil actuator from H2W Technologies, Inc. This actuator's coil can move up and down on linear bearings, and it is centered in its 7.6 mm workspace by a pair of pre-loaded compression springs. Passing current through the coil creates equal and opposite electromagnetic interaction forces on the handle and the coil, which enables us to induce high frequency accelerations on the user's hand. The handle itself is 3D-printed in ABS plastic, and the voice coil actuator is driven by a high bandwidth linear current amplifier.

The endpoints of the master and the slave are each instrumented with a two-axis ADXL320J accelerometer from Analog Devices. This MEMS-based analog accelerometer has a range of ± 5 g (± 49 m/s^2), and its outputs are passed through a first-order analog low pass filter with a cutoff frequency of 500 Hz. A PC running Windows XP and Sensable OpenHaptics 3.0 is used to control the teleoperation system. It operates a servo loop at approximately 1 kHz, measuring the three-dimensional position of each Omni and specifying its three-dimensional force output for each time step. The time step is recorded via high precision counter software provided by [1]. The servo loop also employs a Sensoray 626 card to sample the accelerometers via 16-bit ADC inputs and drive the actuator via a 14-bit DAC output.

To limit the motions used by subjects and simplify the setup, the elbow and gimbal joints of both Omnis are immobilized using physical constraints, as seen in Fig. 2. The shoulder joint's remaining two rotational degrees of freedom allow the handle to move on a spherical surface. As a result, the slave end effector traverses the planar real surface on a one-dimensional arc trajectory. The accelerometer can measure the accelerations that are tangent to and normal to the surface. Both of these signals contain significant high frequency content during exploratory movements, because the tip encounters surface features at a variety of incidence angles. In this study, we chose to focus on matching the slave's tangential accelerations because they were observed to have higher energy than the normal accelerations. Furthermore, our actuator has only one degree of freedom, and we have not yet determined the appropriate method for mapping two-dimensional inputs to this single output axis in real time. Though we believe their larger magnitude makes tangential accelerations more important than those in the normal direction, we acknowledge that this choice is a limiting factor in our study. We are actively investigating this issue and will test it in future human subject studies. For this study, focusing on one-dimensional acceleration matching allows us to compare the efficacy of different matching algorithms without the additional complexities that arise when matching acceleration in two or three dimensions.

3.2 Surface Rendering Algorithms

Eight different surface renderings were developed for the purpose of this study. Each rendering uses different acceleration matching and teleoperation techniques, which make the feedback felt by the user a unique function of the acceleration of the slave end effector and the relative positions of the slave and master. In all cases, the tangential accelerations of the slave end effector were filtered using a digital high pass filter (a fourth-order Butterworth filter) with a cutoff frequency of 20 Hz, yielding the slave acceleration signal a_s. This filter was implemented to prevent the actuator from saturating its output at low frequencies, where it has very little control authority.

All of the teleoperation controllers included a position-forward term, which seeks to make the slave robot track the movement of the master device. The force exerted by the slave motors is thus governed by the following equation:

$$\vec{f}_s = k(\vec{p}_m - \vec{p}_s) + b(\vec{v}_m - \vec{v}_s) + \vec{f}_{gs} \tag{1}$$

Here, $\vec{p}_m$ and $\vec{p}_s$ are the positions of the master and slave, $\vec{v}_m$ and $\vec{v}_s$ are their velocities (computed in real time from the positions), and $\vec{f}_{gs}$ is a gravity compensation force vector. The position gain k was empirically tuned to 150 N/m, and the velocity gain b was set at 0.0005 Ns/m. These values were found to maximize the stiffness on the master handle when the slave is in contact with a hard surface without introducing any buzzing or other perceptible haptic rendering artifacts. The subsections below describe the methods that each of the eight tested algorithms used for computing master force, $\vec{f}_m$, and voice coil actuator force, f_a, during the experiment.

P: Position Feedback

This feedback algorithm implements the second half of a position-position controller, which is the traditional approach to bilateral teleoperation. The master force is determined by the following equation:

$$\vec{f}_m = k(\vec{p}_s - \vec{p}_m) + b(\vec{v}_s - \vec{v}_m) + \vec{f}_{gm} \tag{2}$$

The gains k and b are the same as those for the slave. The master's gravity compensation vector f_{gm} is larger than the slave's since the custom master handle is heavier than the slave end effector. The P algorithm does not include any acceleration feedback, so the auxiliary actuator is not used at all:

$$f_a = 0 \tag{3}$$

DA: Dynamic-gain Acceleration

This algorithm provides only high frequency acceleration feedback, without any low frequency forces. Thus, the master force is just the gravity compensation term:

$$\vec{f}_m = \vec{f}_{gm} \tag{4}$$

This arrangement gives the operator the impression that the surface has a stiffness of zero. Though no low frequency forces are applied by the master Omni, the dedicated voice coil actuator is used to try to vibrate the master handle in the same way that the slave end effector is vibrating. As described above and in [12, 9], this approach uses an approximate model of the system's dynamics (dynamic gain) to compute the actuator force from the slave acceleration, which we will represent as follows:

$$f_a = H_{a\to f}(a_s) \tag{5}$$

The function $H_{a\to f}$ shapes the slave acceleration below 60 Hz and has an approximately constant gain of 0.145 kg (the effective mass of the master handle) above 60 Hz.

P+50%DA: Position plus 50% Dynamic-gain Acceleration

P+DA: Position plus 100% Dynamic-gain Acceleration

P+150%DA: Position plus 150% Dynamic-gain Acceleration

These algorithms combine position feedback (P) with different levels of dynamic-gain acceleration feedback (DA). The equation for master force is given in (2), and actuator force is computed as:

$$f_a = \rho\, H_{a\to f}(a_s) \tag{6}$$

The scalar parameter ρ adjusts the magnitude of the accelerations presented to the user. To understand the effects of both under- and over-actuation, the study tested $\rho = 0.5$, 1.0, and 1.5.

P+CA: Position plus Constant-gain Acceleration

This feedback algorithm is a simplified version of P+DA. Master force is still calculated with (2), but the P+CA algorithm computes the acceleration actuator's output via a constant gain rather than the function $H_{a\to f}$:

$$f_a = m_{mh}\, a_s \tag{7}$$

Here, m_{mh} is 0.145 kg, the effective mass of the master handle. This approach is similar to that taken by [6], and it has a lower computational cost than the algorithms that include dynamic-gain acceleration feedback.

P+OA: Position plus Omni Acceleration

This algorithm attempts to match the slave's high frequency accelerations without using the voice coil actuator. Instead, it adds an acceleration term to the equation for master force, as follows:

$$\vec{f}_m = k(\vec{p}_s - \vec{p}_m) + b(\vec{v}_s - \vec{v}_m) + \vec{f}_{gm} + \gamma\, a_s \hat{j} \tag{8}$$

The scalar parameter $\gamma = 0.1\ kg$ was chosen empirically to produce high frequency accelerations that have a similar magnitude to the input slave acceleration, though the significant device dynamics that intervene between the motors and the handle prevent their frequency content from matching well. To approximate the behavior of the voice coil actuator, this acceleration-dependent force was applied in the vertical direction by multiplying by $\hat{j}$, a unit vector that points upward. This algorithm does not use the voice coil actuator, so (3) applies.

Real: Real Surface

The final feedback algorithm allows the subject to interact with the test surface directly through the handle of the master Omni. The system still runs a position-position controller by implementing (1) and (2), but the auxiliary actuator is not used at all, as specified in (3). Thus the subject feels the contact forces and accelerations generated by direct contact with the real surface, plus the friction and inertia of the master Omni and the bilateral spring and damper connection to the slave Omni. Such an arrangement was chosen to minimize the differences between this condition and the others.

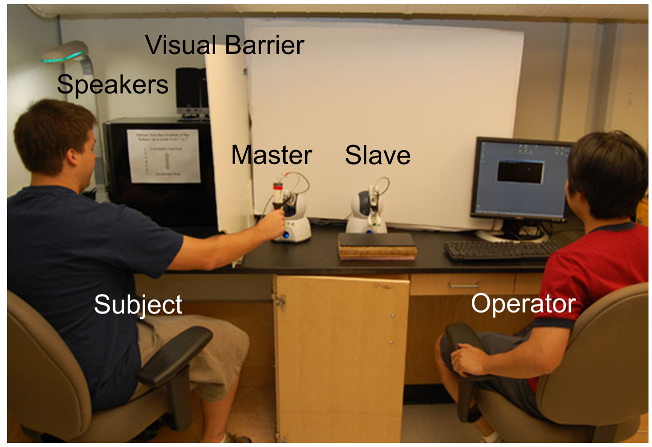

Figure 3: A subject performing our texture rating experiment. The subject (left) reaches around the visual barrier to hold the master stylus, while the operator (right) controls the teleoperation conditions experienced by the user.

4 Study Procedure

Prior to the start of the experiment, subjects were told that they would be participating in a texture rating task involving several different teleoperation algorithms with varying types of feedback. All study procedures were approved by the University of Pennsylvania IRB, and subjects gave informed consent before participating in the study. Subjects were instructed to hold the handle of the master device with a light grasp, and to use it to explore a rendering of the textured surface using a side-to-side scanning motion. The subjects were given no specific instructions on how to explore the surface (i.e., velocity, normal force), but they were warned that the force output capability of the master device was low, so that light contact was preferred.

Each user performed a set of practice trials to become accustomed to the system and to develop a basis for rating the various feedback conditions. The user was allowed to explore each of the eight conditions for as long as he or she liked. They were not told what the individual conditions were, with the exception of the real surface condition. The first condition the user experienced was the real surface, and they were allowed to visually observe the probe tip interacting with that surface alone. Next, a visual barrier was placed between the user and master device (Fig. 3), and we cycled through all seven other teleoperation conditions. During these practice trials no data was recorded.

Next, the user began the real experiment. For each trial, the subject was given six seconds to directly explore the real surface and then six seconds to explore the surface through one of our eight experimental conditions. Pilot testing indicated that six-second trials, while short enough to avoid user fatigue, were long enough for users to fully explore the surface. The user was not informed about which of the eight conditions they were experiencing. The subject was instructed to rate the feel of the rendered surfaces on "realism" by comparing it to the real surface. A seven point scale was used, where one indicated "Completely Not Real" and seven indicated "Completely Real." The handle began each trial several centimeters above the surface in order to allow the experimenter to switch the location of the surface between the master and slave devices. Thus, the user was required to manually lower the probe to the surface at the beginning of each trial. When the real surface was used as a test condition, the user was not informed, and they were still provided with the real surface for six seconds before the rated trial began. Audible beeps were played to signal the beginning and end of each trial, after which the subject was asked to enter his or her rating on a keypad. Throughout the duration of the trials, a pink noise sound was played through computer speakers to mask any sounds produced from the probe-texture interaction or haptic devices. Each subject completed sixteen trials (two random permutations of each of the eight rendering algorithms), which took approximately twenty minutes. In addition to the user's realism rating, we recorded the normal and tangential accelerations, and the positions of both the master and slave devices during each trial, all at a rate of 1 kHz.

After all sixteen trials were completed, we instructed the subject to hold the stylus in the same manner they did during our experiment, and a swept-sinusoid force signal was sent to our linear actuator. By recording the acceleration of the user-held stylus during this test, we are able to identify the dynamics of the stylus-hand system for this user. Upon completion of the experiment, all users were asked to complete a brief optional questionnaire indicating their opinion of what made the various conditions feel more or less real.

5 Results

A total of twelve volunteer subjects participated in the study. Nine of these subjects were male, and three female. Only one user was left handed, but he used his right hand to perform the experiment. Subjects were between the ages of 21 and 36, with a mean age of 25. Their self-reported experience with haptic devices ranged from "none" to "extensive."

Fig. 4 shows a sample of the time-domain data we recorded and analyzed for each trial of the human subject study. The surface penetration and scanning speed describe the behavior of the subject during each trial. The slave accelerations show the response of the surface and the master accelerations show what the user felt. We calculated three quantities for each trial: average surface penetration, average tangential scanning speed, and acceleration feedback performance. These metrics are in addition to the subject's reported realism rating.

For the above four metrics, we used one-way within-subject analysis of variance (ANOVA) to determine whether there were significant differences in the mean of the metric across the different surface rendering algorithms. Additionally, we performed post-hoc pairwise comparisons to test the null hypothesis that the mean difference of the metric between two rendering algorithms is zero. We choose $\alpha = 0.05$ to determine significance, and we use the Bonferroni correction to adjust this level down to α/n, where $n = 28$ is the number of comparisons being made. We also report effect sizes using η^2.

5.1 Penetration Depth

Penetration depth is defined as the vertical position difference between the master handle and the slave end-effector when it is touching the surface for the haptic rendering conditions. In other words, this metric defines how far into the rendered surface the user has lowered the handle. Under position-position control some surface penetration is required in order for this device to exert a normal low frequency force upon the user's hand. If the stiffness was higher, penetration depth would likely decrease.

Fig. 5 shows a box plot of mean surface penetration across subjects for the eight surface renderings. One-factor within-subject ANOVA on the mean surface penetration reveals a large significant effect of surface rendering type ($F(7) = 39.88, p < 0.0001, \eta^2 = 0.6509$). Subject also has a small significant effect ($F(11) = 6.61, p < 0.0001, \eta^2 = 0.1696$). Post-hoc pairwise comparisons, visualized in Fig. 6, indicate that the Real surface is significantly different from all the other renderings in mean surface penetration. Similarly, the DA rendering is significantly different from all others. No significant differences are found in pairwise comparison of any of other rendering methods.

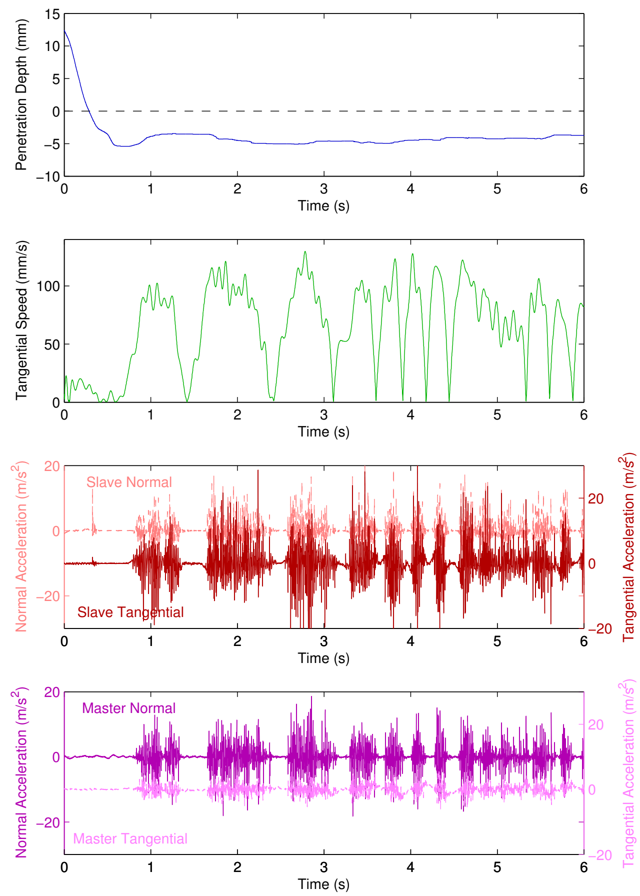

Figure 4: Sample recorded time-domain trial data: Subject 10, condition P+DA, first repetition. Average tangential speed of surface exploration was 67.8 mm/s, average penetration depth was 4.52 mm, and the realism rating was 6 out of 7. In P+DA mode normal accelerations on the master are made to track tangential accelerations on the slave via the linear voice-coil actuator.

5.2 Scanning Speed

Scanning speed is defined as the tangential speed at which the user moved the master handle along the textured surface during contact.

Fig. 7 shows a box plot of mean scanning speed for the eight surface renderings across subjects. One-factor within-subject ANOVA on the mean scanning speed reveals a negligible significant effect of surface rendering type ($F(7) = 2.52, p = 0.0219, \eta^2 = 0.0331$). On the other hand, subject has a large significant effect ($F(11) = 39.74, p < 0.0001, \eta^2 = 0.8220$). Though surface was found to be a significant main effect, post-hoc pairwise comparisons indicate that there is no significant differences in mean scanning speed across any of the different surface renderings.

5.3 Acceleration Feedback Performance

In order to evaluate the acceleration feedback acceleration feedback of the various rendering methods, we use a performance metric P_{am} defined by the RMS error between the frequency-domain amplitudes of the slave and master signals over the course of the trial normalized by the RMS of the recorded signal's frequency-domain amplitude:

$$P_{am} = 1 - \frac{RMS(DFT\{a_s\} - DFT\{a_m\})}{RMS(DFT\{a_s\})} \tag{9}$$

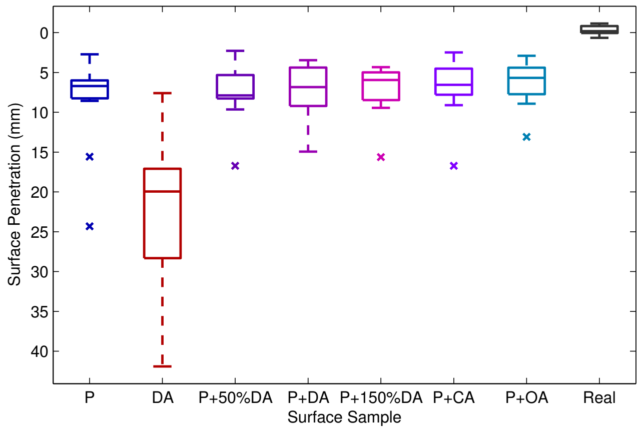

Figure 5: Box plot of the subject's mean surface penetration depth for each of the eight surface renderings. In each box, the center line indicates the median, the top the third quartile, and the bottom the first quartile. The whiskers extend to the furthest data value that is not considered a probable outlier. Probable outliers, marked as (x)'s, are defined as those values further away from the median than 1.5 times the range first or third quartiles.

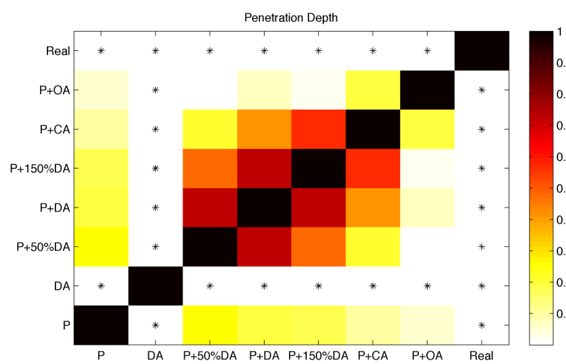

Figure 6: Post hoc pairwise t-tests of penetration depth for the eight different surface rendering algorithms. Significant difference, defined by $\alpha = 0.05$ and a Bonferroni correction of 28, is indicated by a (*). P-value is indicated by color.

This metric provides an indication of the quality of the frequency-domain match between the slave and master accelerations, a_s and a_m, which we believe to be a perceptually relevant measure. Fig. 8 shows the magnitude of the discrete Fourier transform of both the slave and master accelerations for the sample trial of Fig. 4.

Fig. 9 shows box plots of mean scanning speed for the eight surface renderings across subjects. One-factor within-subject ANOVA on the mean acceleration feedback performance reveals a large significant effect of surface rendering type $(F(7) = 584.01, p < 0.0001, \eta^2 = 0.9635)$. Subject also has a negligible significant effect $(F(11) = 7.1, p < 0.0001, \eta^2 = 0.0184)$. Post-hoc pairwise comparisons indicates that there is significant difference in mean acceleration feedback performance for all combinations of pairs, except for between P+50%DA and P+OA.

5.4 Realism Rating

Fig. 10 shows a box plot of mean realism rating for the eight surface renderings across subjects. One-factor within-subject ANOVA on the mean realism rating reveals a large significant effect of surface rendering type $(F(7) = 48.29, p < 0.0001, \eta^2 = 0.7227)$. Subject also has a small significant effect $(F(11) = 4.79, p < 0.0001, \eta^2 = 0.1126)$. Post-hoc pairwise comparisons, visualized in Fig. 11, indicate that the Real surface is significantly different from all the other renderings, with respect to mean realism rating. Additionally, P+DA, P+150%DA, P+CA, and P+OA show no significant differences with one another. Similarly, there is no significant difference between P and DA, and there are significant differences between these two renderings and all others. P+50%DA shows significant differences only with P, P+DA, and Real.

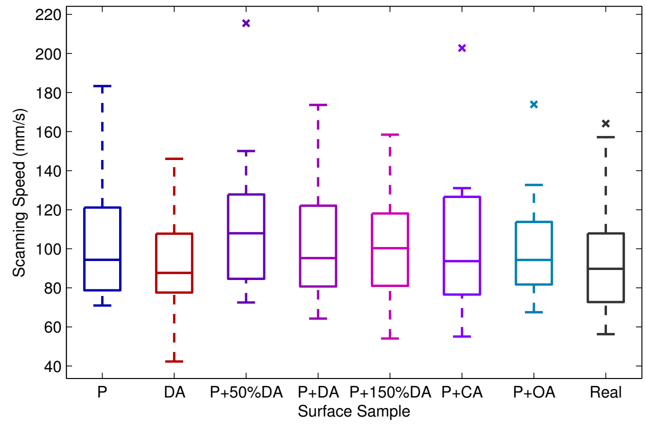

Figure 7: Box plot of the subject's tangential scanning speed for each of the eight surface renderings.

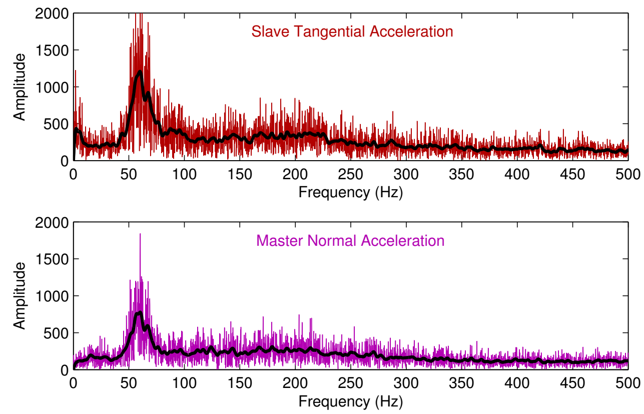

Figure 8: Sample frequency-domain view of the acceleration signals: Subject 10, Condition P+DA, First repetition. The acceleration feedback performance for this trial is 67.1%.

6 Discussion

The analysis of penetration depth in Figs. 5 and 6 shows that acceleration feedback did not have a significant effect on the normal force exerted by the user during exploration of the surface. Penetration depth was only influenced by the rendered stiffness of the surface. In post-test surveys many subjects mentioned that they believe that surface stiffness had a major effect on their perceived realism of a surface, but without a more detailed study of penetration depth versus rated realism, no definitive conclusions can be drawn.

The analysis of scanning speed, in Fig. 5 shows that different users chose a wide variety of different speeds, and that users tended to maintain a consistent scanning speed from trial to trial. Thus, surface rendering methods did not have a significant effect on the speed at which users scanned the surface.

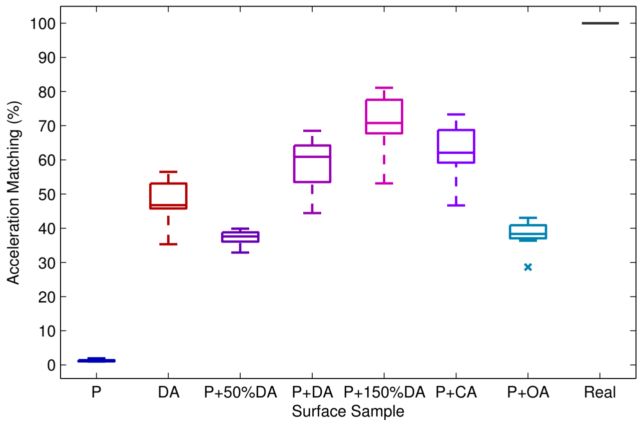

Figure 9: Box plot of the acceleration feedback performance for each of the eight surface renderings.

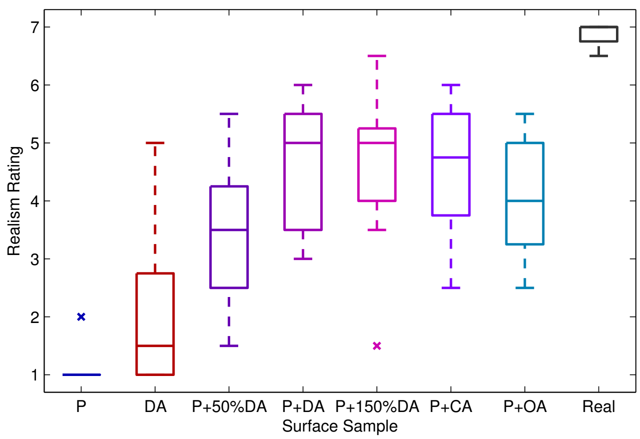

Figure 10: Box plot of the realism ratings for each of the eight surface renderings.

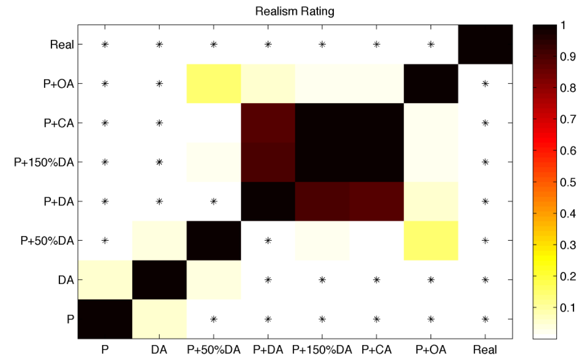

Figure 11: Post hoc pairwise t-tests of realism rating for the eight different surface rendering algorithms. Significant difference, defined by $\alpha = 0.05$ and a Bonferroni correction of 28, is indicated by a (*). P-value is indicated by color.

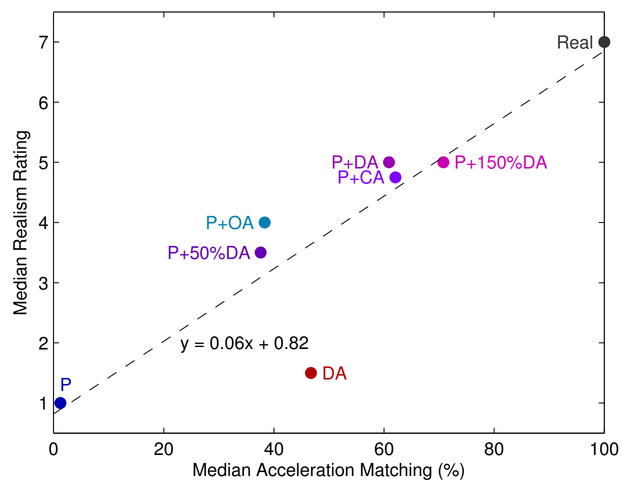

Figure 12: Linear regression between median realism ratings and median acceleration feedback performances.

Analysis of acceleration feedback performance (Fig. 9) indicates that this metric was largely subject independent. Additionally the fact that P+150%DA performed significantly better than P+DA indicates that the approach described in [12, 9] may have a tendency to underactuate accelerations. This suggests there is a need to improve the fidelity of our dynamic model of the system.

The analysis of realism ratings (Figs. 10 and 11) indicates that adding high frequency acceleration feedback to position feedback in any of its many forms (P+50%DA, P+DA, P+150%DA, P+CA, P+OA) is a significant improvement over low frequency position feedback only (P). However, there is still considerable room for improvement as the realism of even our best surface rendering method, P+150%DA, remains significantly below the realism of the Real surface. The fact that P+50%DA is significantly worse than P+DA seems to indicate that underactuation of acceleration feedback has a detrimental effect on perceived realism.

Observation of the box plots for acceleration feedback and realism rating, Figs. 9 and 10, suggests that there is a relationship between acceleration feedback performance and realism rating. Plotting these two metrics against each other, Fig. 12, reveals a strong positive linear correlation for the medians ($R^2 = 0.7844$ and $p = 0.0034$). One obvious outlier to this linear correlation is the DA surface rendering method, which receives a much lower realism rating due to its lack of any surface stiffness. Holding surface stiffness constant (i.e., neglecting Real and DA) results in an even stronger positive linear correlation for the medians ($R^2 = 0.952$ and $p = 0.0009$).

This finding supports our choice of acceleration feedback performance metric, which quantifies the closeness of match of the magnitudes of the discrete Fourier transform of the slave and master accelerations. It also suggests that given constant stiffness, acceleration feedback performance may be a good predictor of perceived realism, at least in the context of our physical setup and a texture realism rating task.

We found it surprising that P+OA performed as well as it did in terms of both acceleration feedback performance and rated realism, given the problems this class of haptic device has with high frequency acceleration feedback (Section 2). We did encounter several drawbacks associated with base-motor actuation. Setting the gain for the P+OA acceleration controller was challenging due to its empirical and subjective nature. Additionally, the fidelity of the high frequency feedback was lacking; accelerations that we intended to be played only along the y-direction of the Omni would instead cause vibration in all directions with a resonance at approximately 200 Hz. This rendering mode also seemed to overdrive the motors, causing premature heating. For these reasons we still believe that the best option in high performance applications is to augment traditional haptic devices with a high frequency acceleration actuator.

7 Conclusions and Future Work

Through the study of haptic device design and human psychophysics, many researchers have come to suspect that high frequency accelerations are critically important for the human perception of real textures. To our knowledge this paper is the first study to quantify the effect of these high frequency signals on the perceived realism of remotely probed textures. Through careful experimentation and analysis we have shown that incorporating acceleration feedback (P+DA, P+CA, P+OA, etc.) into traditional haptic algorithms significantly enhances the perceived realism of the interaction. Furthermore, for the experimental setup in this study, we have demonstrated a linear correlation between acceleration feedback quality and perceived realism when some minimal value of surface stiffness is present.

The best vibration-augmented samples earned a median realism rating of about 5 out of 7, while position-position control received a 1 out of 7. While promising, none of the teleoperation controllers achieved a realism level as high as the 7 given to the real surface, showing that there is still room for improvement in the design of acceleration-feedback systems. We are currently working to increase the tracking performance of our dynamic-gain acceleration algorithm by improving our dynamic model of the system and adding local closed-loop feedback from the accelerometer on the master.

Our current implementation focuses on matching a single acceleration axis on the master to one on the slave, but we are researching more complex ways of combining the three-dimensional acceleration vector recorded by the slave into one signal for actuation on the master. By better matching the combined acceleration power of the three slave axes, we believe we can achieve even higher realism ratings. While this study was carried out with teleoperated devices, it is likely that these results also apply to virtual environments, and that generating high frequency acceleration signals in simulation will result in similar gains in perceived realism, a current topic of research in our laboratory. In the future we hope to perform a follow up user study with more systematically varied surface parameters in order to develop a better model of human realism perception.

Acceleration matching algorithms such as the constant gain Omni acceleration (P+OA) are simple to implement on existing haptics hardware (computationally efficient, low-cost), and very effective in enhancing the user experience. For demanding applications even higher levels of realism can be achieved through the use of a dedicated handle actuator. We believe this work is a strong step toward showing that accurately rendering high frequency acceleration content is of critical importance for a haptic device attempting to display realistic interactions with textured surfaces.

Acknowledgements

The authors wish to thank the members of the Penn Haptics Group for their support and inspiration. This work was supported by the University of Pennsylvania and the National Science Foundation (IIS-0845670).

References

[1] J. Barbič. Computer graphics research code, http://www.jernejbarbic.com/code, 2009.

[2] J. Bell, S. Bolanowski, and M. H. Holmes. The structure and function of Pacinian corpuscles: A review. *Progress in Neurobiology*, 42(1):79–128, Jan. 1994.

[3] G. Campion and V. Hayward. Fundamental limits in the rendering of virtual haptic textures. In *Proc. IEEE World Haptics Conference*, pages 263–270, Mar. 18–20, 2005.

[4] S. Choi and H. Z. Tan. Perceived instability of virtual haptic texture: I. experimental studies. *Presence: Teleoperators and Virtual Environments*, 13(4):395–415, 2004.

[5] N. Diolaiti, G. Niemeyer, F. Barbagli, J. K. Salisbury, and C. Melchiorri. The effect of quantization and Coulomb friction on the stability of haptic rendering. In *Proc. IEEE World Haptics Conference*, Mar. 2005.

[6] D. A. Kontarinis and R. D. Howe. Tactile display of vibratory information in teleoperation and virtual environments. *Presence: Teleoperators and Virtual Environments*, 4(4):387–402, Aug. 1995.

[7] K. J. Kuchenbecker, J. Fiene, and G. Niemeyer. Event-based haptics and acceleration matching: portraying and assessing the realism of contact. In *Proc. IEEE World Haptics Conference*, pages 381–387, Mar. 18–20, 2005.

[8] K. J. Kuchenbecker, J. P. Fiene, and G. Niemeyer. Improving contact realism through event-based haptic feedback. *IEEE Transactions on Visualization and Computer Graphics*, 12(2):219–230, March/April 2006.

[9] K. J. Kuchenbecker, J. M. Romano, and W. McMahan. Haptography: Capturing and recreating the rich feel of real surfaces. To appear In Proceedings of the 14th International Symposium of Robotics Research (ISRR 09), Lucerne, Switzerland, Aug. 31-Sept. 3 2009.

[10] S. J. Lederman and R. L. Klatzky. Hand movements: A window into haptic object recognition. *Cognitive Psychology*, 19:342–368, 1987.

[11] W. McMahan and K. J. Kuchenbecker. Displaying realistic contact accelerations via a dedicated vibration actuator. In *Proc. IEEE World Haptics Conference*, pages 613–614, Mar. 18–20, 2009.

[12] W. McMahan and K. J. Kuchenbecker. Haptic display of realistic tool contact via dynamically compensated control of a dedicated actuator. In *Proc. IEEE/RSJ International Conference on Intelligent Robots and Systems*, pages 3171–3177, Oct. 10-15 2009.

[13] A. M. Okamura, M. R. Cutkosky, and J. T. Dennerlein. Reality-based models for vibration feedback in virtual environments. *IEEE/ASME Transactions on Mechatronics*, 6(3):245–252, Sept. 2001.

[14] C. Salisbury, R. B. Gillespie, H. Tan, F. Barbagli, and J. K. Salisbury. Effects of haptic device attributes on vibration detection thresholds. In *Proc. IEEE World Haptics Conference*, pages 115–120, Mar. 18–20, 2009.

[15] S. A. Wall and W. Harwin. A high bandwidth interface for haptic human computer interaction. *Mechatronics*, 11(4):371–387, June 2001.